Transverse patterns in a laser with an injected signal

Stefano Longhi*
Research Laboratory of Electronics, Massachusetts Institute of Technology, Cambridge, Massachusetts 02139
(Received 3 February 1997; revised manuscript received 27 May 1997)

Pattern formation near threshold in large-aspect-ratio, single-longitudinal-mode, two-level lasers with plane mirrors under the action of a weak injected plane-wave field resonant with the atomic transition frequency and tilted with respect to the laser cavity axis is analytically investigated in terms of the amplitude equations for the system. It is shown that, when the laser emission occurs off-axis, the appearance of resonances among the injected signal field and the unstable emerging tilted waves drastically changes the pattern selection properties of the free-running laser. As a result new transverse patterns, which include singly and doubly periodic stripes and undulating hexagons, may be stabilized by the injected signal. These patterns arise from the superposition of the forced mode with either one, two, or three traveling waves on the critical circle of the free-running laser. This is a distinctive feature from similar structures more commonly found in passive optical systems, where complex patterns always arise as a superposition of standing waves. The stability properties of the various patterns and their selection rules are analytically investigated within the amplitude equations.
[S1050-2947(97)11009-5]

PACS number(s): 42.65.Sf, 42.60.Mi

I. INTRODUCTION

Spontaneous pattern formation in nonlinear optics has been the subject of extensive investigations in recent years [1]. Coupling of diffraction with an optical nonlinearity in two transverse spatial dimensions has revealed the appearance of transverse patterns both in passive [2–5] and active [6–14] optical systems, including Kerr-like systems with two-dimensional feedback [2–5], lasers [6–9], photorefractive oscillators [10,11], optical parametric oscillators [12–14], and others (a more complete list of references can be found in the editorial introduction of Ref. [1]). The kinds of patterns that can emerge in an optical system depends crucially on the *aspect ratio* of the system [11]. In a cavitylike configuration (as in lasers), the aspect ratio is typically determined by the Fresnel number of the optical cavity [11]. In small-aspect-ratio systems, pattern formation is controlled by the geometrical boundaries (e.g., spherical mirrors of the cavity) and the spatiotemporal dynamics typically involves few cavity modes [6]. Conversely, in large-aspect-ratio systems, usually obtained by considering plane mirrors and uniform pumping, pattern formation is independent of the transverse boundaries and is thus likely to be the result of nonlinear bulk effects. There are essentially two approaches to studying pattern formation in large-aspect-ratio systems that complement each other [15]. The first one is based on the derivation of *order-parameter equations* (like the complex Ginzburg-Landau and the Swift-Hohenberg equations) capable of capturing the nonlinear dynamics of the system under suitable limits [15]. As these equations have a universal form (i.e., independent of the original equations specific for the particular physical problem), they provide a connection between pattern formation in nonlinear optics and in other physical fields. The second method is based on the derivation of the *amplitude equations* for the system near the instability point. These equations are able to predict the existence of certain patterns which reflect the symmetry of the bulk parameters. A common situation is that where the rotational symmetry in the transverse plane introduces a continuous degeneracy of critical modes, so that only the modulus (but not the direction) of their wave vectors is fixed by the system parameters. In this case the critical modes lie on a set of circles (called *critical circles*) in the wave-vector space whose number corresponds to that of the unstable bands in the linearized problem. Although, at linear instability, all these modes may grow, due to their competition only a few of them typically survive and saturate, leading to the formation of regular spatial structures. The most common patterns which are observed when competition of critical modes is restricted to a single unstable band are tilted (or traveling) waves, stripes, squares, triangles, and hexagons [2–4,7,9,16]. The nature of the selected patterns depends crucially on the nonlinear terms in the amplitude equations and thus on the intrinsic symmetry of the problem [15]. As a general rule, it turns out that stripes and hexagons are likely whenever second-order nonlinear terms arise in the amplitude equations (as, for example, in optical bistability [4,17,18] and in Kerr-like systems with a single-feedback mirror [2,3]), whereas tilted waves and square (or rhombic) vortex lattices are commonplace when only third-order nonlinear terms are present in the amplitude equations (as, for example, in lasers [7,9] and nondegenerate optical parametric oscillators [13]). Furthermore, it turns out that passive optical systems usually give rise to a richer variety of patterns and bifurcations than active systems. In this regard, many recent works have revealed both experimentally and theoretically that, besides rolls, triangles, and hexagons [3,4], passive Kerr-like optical systems with two-dimensional feedback are capable of generating a wide variety of other regular patterns which were known in hydrodynamics [19–21], such as quasipatterns with N-fold orientational order [5,22–24], multiconical emission [23–26], coexistence of patterns with different

*Present address: Dipartimento di Fisica, Politecnico di Milano, Piazza L. da Vinci 32, 20133 Milano, Italy.

symmetry [27], and mixed Hopf-Turing structures [28]. In particular, quasipatterns arising from the interaction of modes belonging to the same unstable band have been experimentally observed in a liquid-crystal light valve system with field rotation [22], and theoretically predicted in a single-feedback mirror device with rubidium atoms [5]. The pattern scenario is further enriched when modes belonging to different unstable bands become simultaneously critical (multiconical emission). In this case the cooperative mode dynamics among modes belonging to different bands may lead to stable quasipatterns [19,23,25,26]. However, in general it turns out that such an intermode coupling can occur only for very particular parameter values [19,23], and it requires mutual phase locking of all modes [26]; otherwise multiconical emission in the near field manifests itself as a tiling consisting of domains with different spatial periodicity [27]. The single-feedback mirror system with a thin two-level medium [28] also represents an example in nonlinear optics of pattern-forming system capable of supporting mixed Turing-Hopf patterns. In that case the patterns originate from a triadic resonance among Hopf and Turing modes that become simultaneously critical [28]; as an Hopf instability is involved, these patterns drift. When considering active optical systems, such as lasers [7–9] and other systems where gain is not provided by population inversion (such as optical parametric oscillators [12,13] and photorefractive oscillators [10,11]), their pattern scenario seems much simpler than that discussed above, at least close to threshold and whenever boundary effects are negligible. In particular, it has been shown that these systems may generate similar patterns [10,13] which involve modes belonging to only one critical circle, the absence of higher unstable bands being a consequence of the uniform-field model which is usually valid for those systems. An important and distinctive feature of lasers (and of the other active systems quoted above) from all the passive optical systems previously discussed is that the elementary critical mode, which is the basic pattern needed to build more complex patterns, is a single traveling (or tilted) wave (TW) on the critical circle [7]. Conversely, in passive systems it turns out that the elementary pattern is never a single TW, but a roll pattern obtained as a superposition of two counterpropagating TW's having the same intensity (see, for instance, Ref. [16]). Therefore, in lasers one would expect *a priori* the possibility of generating patterns that do not have analogous in passive systems (for instance, patterns formed by the superposition of an odd number of TW's, or of oppositely oriented TW's with different amplitudes). Nevertheless it is well known that for the single-longitudinal-mode, free-running laser with a longitudinal cavity frequency smaller than the atomic resonance one, a single tilted wave is a global attractor of the laser equations and it is able to dominate and to suppress all others; in particular, two or three tilted waves may not be simultaneously excited due to the absence of second-order nonlinear terms in the amplitude equations [7,8]. At most two couples of oppositely oriented, out-of-phase TW's (alternating rolls) may be stabilized by the nonlinearity, which gives rise to rhombic patterns [9]. It is clear that pattern selection properties of the free-running laser could drastically change if the inversion symmetry of the amplitude equations (which is intrinsic of the laser equations) is somehow broken. This may be achieved by injection of a signal field into the laser cavity. Lasers with an injected signal are quite popular systems in laser physics, and they display a rich variety of nonlinear phenomena [29]; the study of transverse effects in these systems has been considered recently [30,31], but they did not attract as much attention as other systems, mainly because signal injection did not seem to enrich the pattern formation properties of the free-running laser. In Ref. [30] the derivation of an order-parameter equation for the laser field near threshold in the presence of a weak injected plane-wave signal was presented in various limiting cases. That analysis was mainly restricted to the case where the excited longitudinal cavity frequency is larger than the atomic resonance frequency, which prevents off-axis emission for the laser radiation. In that case a complex Ginzburg-Landau equation for the order parameter was derived by the use of a multiple scale perturbation approach. The opposite case was not so extensively studied, and a brief analysis was given in Ref. [31], where it was shown for the one-dimensional case that the excitation of a single tilted wave for the laser equations is also likely when a weak signal is injected into the laser cavity. From the viewpoint of pattern formation, signal injection does not seem therefore to enrich substantially the free-running laser dynamics. That analysis, however, assumes implicitly that the frequency of the injected signal is different from the atomic resonance frequency, which is exactly the frequency of the emerging tilted wave.

In this paper we investigate the problem of pattern formation and selection near threshold in a laser with a weak injected signal, by use of the amplitude equations approach in the case where the laser emission occurs off-axis and the frequency of the injected signal is exactly tuned to the frequency of the atomic transition. Furthermore, we consider a plane-wave injected field tilted with respect to the axis of the laser cavity, and discuss how the pattern formation properties change as the tilting angle is varied and the pumping parameter of the laser is increased. As the injected signal is weak, the linear instability of the laser equations is ruled as for the free-running case, and the critical modes are TW's on the critical circle. Nevertheless, it is shown that the existence of the injected signal with the same frequency as that of the emerging tilted waves drastically changes the free-running laser dynamics with the appearance of new kind of patterns and a rich bifurcation scenario even near threshold, where the validity of the amplitude equations is restricted. This occurs as the injected signal introduces in the amplitude equations for the neutral modes new interactions ruled by precise resonance conditions involving four-wave vectors that are responsible for the emergence of transverse patterns. In particular, stable patterns involving simultaneous excitation of one, two, or three tilted waves may appear. This is a distinctive feature with respect to the optical bistability model, where pattern formation always involves the simultaneous emission of two oppositely oriented traveling waves (rolls) [4]. It turns out that a key parameter which governs the pattern forming properties is the ratio between the wave number k_C of the neutral modes and that k_0 of the injected field, which depends upon the tilting angle. The other important parameters controlling the patterns are the pump parameter for the atoms and the amplitude of the injected signal, which may lead to further bifurcations. In particular, it turns out

that at high values of the pump parameter the stable patterns involve only one tilted wave, thus recovering the limit of a laser without injected signal, whereas for high values of the injected field the laser emission occurs on the forced mode.

The paper is organized as follow. In Sec. II we describe the laser model with a weak injected signal, and derive the amplitude equations for the neutral modes which describe the laser dynamics close to threshold. In Sec. III we present a set of solutions of the amplitude equations involving $N=1$, 2, or 3 modes, and investigate their stability properties. In Sec. IV a summary of the pattern formation and selection rules is presented, and, finally, in Sec. V the main conclusions are outlined.

II. DESCRIPTION OF THE MODEL AND DERIVATION OF THE AMPLITUDE EQUATIONS

We consider a single-longitudinal-mode, homogeneously broadened two-level laser with plane mirrors of infinite transverse extension and uniform pumping, with an injected plane-wave signal field resonant with the atomic transition frequency. In general we will assume that the injected field is tilted with respect to the laser cavity axis. The starting point of the analysis is provided by the usual Maxwell-Bloch laser equations which, in the paraxial and mean-field approximations, may be written in the following dimensionless form [8,30]:

$$\partial_t e - ia\nabla^2 e - i\Omega e = -\sigma e + \sigma p + E\ \exp(i\mathbf{k}_0\cdot\mathbf{x}) \quad (1a)$$

$$\partial_t p + p = (r-n)e, \quad (1b)$$

$$\partial_t n + bn = \tfrac{1}{2}(e^* p + p^* e), \quad (1c)$$

where e and p are the scaled envelopes of the electric and polarization fields referenced to the atomic resonance frequency; n is proportional to the difference between the atomic inversion and the initial inversion; a is the diffraction parameter; r is the pump parameter; σ and b, respectively, are the decay rates of the electric field and of the population inversion, both scaled to the decay rate of the polarization; $\nabla^2=\partial_x^2+\partial_y^2$ is the transverse Laplacian; t is the time variable scaled to the decay time of the polarization; the detuning parameter Ω is the difference between the atomic and the longitudinal cavity frequencies, divided by the polarization decay rate; E is proportional to the amplitude of the injected plane-wave field; $\mathbf{k}_0$ is the wave-vector component of the injected field transverse to the cavity axis; and $\mathbf{x}=(x,y)$. Here we consider the case of a weak injected field by assuming in Eq. (1a) that $E=E_0\varepsilon$, ε being a small parameter. As a consequence, at leading order in ε the dynamics described by Eqs. (1) exactly coincide with that previously studied in Ref. [7] for a two-level laser model in absence of the injected signal. In particular, it is known that for a positive detuning parameter the laser threshold is reached at $r=1$ and the neutral modes at threshold are tilted waves with transverse wave vector $\mathbf{k}$ such that $|\mathbf{k}|=k_C\equiv(\Omega/a)^{1/2}$ (Turing instability), whereas for a negative detuning parameter the threshold is reached at $r=(1+\Omega^2)^{1/2}$ and the bifurcating mode is oscillatory in time but homogeneous in space [7]. As we are interested on the formation of certain patterns, we will limit our analysis to the positive detuning case. Furthermore, as we want to study the influence of the injected signal field on the nonlinear selection mechanism of the neutral modes, we consider a pump parameter r close to its threshold value by assuming $r=1+\varepsilon^2$. Such a dependence of r on ε will become clearer later, and it essentially ensures that the amplitudes of the bifurcating modes and of the injected field in the cavity be of the same order of magnitude [30]. This scaling fails in the singular limit $k_0=k_C$, which is not, however, of particular interest from the point of view of transverse patterns and therefore will be not considered here [32]. The derivation of the amplitude equations is based on a standard weakly nonlinear analysis of Eqs. (1) similar to that developed in Ref. [30], and consists of looking for a solution of the equations as a power expansion in ε,

$$\mathbf{v}=\varepsilon\mathbf{v}^{(1)}+\varepsilon^2\mathbf{v}^{(2)}+\varepsilon^3\mathbf{v}^{(3)}+\cdots, \quad (2)$$

where $\mathbf{v}=(e,p,n)^T$ contains the field matter variables. The introduction of slow space and time variables follows from a straightforward analysis of the linear problem, which is discussed in Ref. [7]. As we are mainly interested in the existence of certain patterns arising from the interaction of a finite number of critical modes, we will neglect finite bandwidth effects, so that no slow spatial variables are introduced. In this case, only one slow time variable, given by $T=\varepsilon^2 t$, is needed to capture the slow time evolution of the mode amplitudes [7]. In order to proceed into the perturbation expansion, the order of magnitude of the decay rates b and σ of the population inversion and electric field scaled to the polarization decay rate should be stated. Here we give an explicit derivation of the amplitude equations in the case of class-C lasers, where all damping rates are comparable in magnitude [8], so that we may assume in the perturbation expansion $b=O(1)$, $\sigma=O(1)$; a similar analysis, however, could be done for class-A lasers, where both material polarization dephasing and population decay rates are much larger than the cavity field damping rate [8]. By substituting expansion (2) into Eqs. (1), using the derivative rule $\partial_t=\varepsilon^2\partial_T$ and setting $r=1+\varepsilon^2$, and $E=E_0\varepsilon$, a hierarchy of equations for successive corrections to $\mathbf{v}$ is obtained. The solution at leading, $O(\varepsilon)$, is $\mathbf{v}^{(1)}=(e^{(1)},e^{(1)},0)^T$, where $e^{(1)}$ is given by an arbitrary linear combination of neutral modes at threshold plus a forced mode arising from the injected signal, namely,

$$e^{(1)}=A_0\exp(i\mathbf{k}_0\cdot\mathbf{x})+\sum_{l=1}^{N}A_l\exp(i\mathbf{k}_l\cdot\mathbf{x}), \quad (3)$$

with $|\mathbf{k}_l|=k_C$. In Eq. (3), A_l ($l=1,2,3,\ldots,N$) are arbitrary complex functions of the slow time scale T, whereas A_0 is the amplitude of the forced mode, which is given by

$$A_0=\frac{iE_0}{\Omega-ak_0^2}. \quad (4)$$

Because of the rotational symmetry in the transverse plane, the choice of the linear combination of neutral modes has been left arbitrary at this stage. The solution at $O(\varepsilon^2)$ may be chosen as $\mathbf{v}^{(2)}=(0,0,(1/b)|e^{(1)}|^2)^T$, whereas at $O(\varepsilon^3)$ solvability conditions determine the slow time evolution of the amplitudes A_l, which explicitly read

$$(1+\sigma)\partial_T A_l=\sigma A_l-\frac{\sigma}{b}\sum_{m,r,s=0}^{N} A_m A_r A_s^{*}\delta_{\mathbf{k}_m+\mathbf{k}_r-\mathbf{k}_s-\mathbf{k}_l} \tag{5}$$

$(l=1,2,3\ldots,N)$. Introducing the new variables $\tau=t(1+\sigma)^{-1}\sigma$ and $B_l=\varepsilon b^{-1/2}A_l$, and observing that $\partial_\tau=\sigma^{-1}(1+\sigma)\varepsilon^2\partial_T$, $\varepsilon^2=r-1$, we finally obtain the *amplitude equations*

$$\partial_\tau B_l=(r-1)B_l-\sum_{m,r,s=0}^{N} B_m B_r B_s^{*}\delta_{\mathbf{k}_m+\mathbf{k}_s-\mathbf{k}_s-\mathbf{k}_l},$$

$$(l=1,2,3,\ldots,N), \tag{6}$$

where

$$B_0=\frac{iE}{\sqrt{b}(\Omega-ak_0^2)}. \tag{7}$$

Equations (6) represent the starting point of our analysis of pattern formation in a laser with injected signal. It should be noted that the amplitude of the forced mode, B_0, is fixed by the external injected signal according to Eq. (7); nevertheless it enters into the nonlinear dynamics of the amplitudes of the other modes, and may introduce new resonances, as we will discuss in Sec. III. Furthermore, the phase of B_0 does not play an important role in the pattern formation process, and with a suitable redefinition of the phase of the injected signal amplitude E we may assume B_0 to be a real and positive number.

III. TRANSVERSE PATTERNS AND THEIR STABILITY

The amplitude equations (6) may have, in general, different families of solutions involving a different number N of modes, which correspond to different patterns in the transverse plane of the cavity axis. In particular, the observable of major interest in an experiment is the laser output intensity profile, which turns out to be proportional to the time average of the square of the electric field. From Eq. (3), the near-field intensity at leading order is given by

$$I=\left|\alpha\ \exp(i\mathbf{k}_0\cdot\mathbf{x})+\sum_{l=1}^{N} B_l\exp(i\mathbf{k}_l\cdot\mathbf{x})\right|^2, \tag{8}$$

where for clarity here and in the following we will denote by α the amplitude (real and positive) of the forced mode, given by Eq. (7). The resultant pattern will therefore depend on the interference among the forced mode solution and the tilted waves which are neutral at threshold. Although in principle at the linear instability many modes can be excited, owing to their nonlinear interactions only few of them survive leading to a stable pattern [15]. Furthermore, the wave vectors of the surviving modes do not have an arbitrary geometry, but are typically arranged in such a way as to satisfy simple algebraic conditions, which depend upon the nature of the nonlinearities in the amplitude equations and reflect the intrinsic symmetry of the system. In the case where no signal is injected into the cavity, i.e., for $\alpha=0$, it is known that the amplitude equations (6) may support only one mode (tilted or traveling wave), which gives a uniform intensity profile at the output [7], or four modes composed by two couples of rolls (two traveling waves with opposite wave vectors) with phase alternation (alternating rolls, or alternating standing waves), which correspond to a square (or rhombic) vortex lattice in the transverse laser intensity [9]. In particular, solutions of the amplitude equations involving two or three tilted waves are always unstable in the laser case. These features are not substantially modified when a weak signal is injected into the laser cavity, provided that it is detuned in frequency from the emerging modes. In this case the laser emission occurs on a single tilted wave which is superimposed on the forced mode; this gives rise to traveling rolls [21]. When the injected signal is resonant in frequency with the tilted waves, which is our case, new resonances appear in the amplitude equations which drastically change the mode-mode interaction among TW's on the critical circle. In this section we consider solutions of the amplitude equations (6) involving $N=0$, 1, 2, or 3 modes, and study their stability. The $N=0$ solution corresponds trivially to the forced state (homogeneous intensity in the transverse plane), and its instability gives rise to formation of patterns. The $N=1$ state, where only one tilted wave is excited, gives rise to a stripe pattern whose orientation and spatial periodicity depends on the angle between $\mathbf{k}_0$ and the wave vector of the excited mode, which may be arbitrary. For brevity we will call this state $\mathbf{S}_1$. The $N=2$ state gives rise to stripe patterns too, but in this case the orientation of the stripes is parallel to $\mathbf{k}_0$, and a single or double spatial periodicity of the stripes may occur. We will call this state $\mathbf{S}_2$. Finally, the $N=3$ state, which involves three tilted waves, gives rise to undulating hexagonal patterns. It should be noted that the limiting case, where the injected signal is orthogonal to the plane cavity mirrors, introduces a rotational symmetry of the problem in the transverse plane which, on the contrary, is broken when the injected signal is tilted with respect to the cavity axis. Such symmetry is responsible for the appearance of special triadic resonances in the amplitude equations, and this case needs therefore a separate analysis that will be given elsewhere.

A. Forced (homogeneous) solution ($N=0$)

The amplitude equations (6) admit the trivial zero solution $B_l=0$ $(l=1,2,\ldots,N)$, which corresponds to the laser emission in the forced mode. To study the stability of this solution, we linearize Eqs. (6) around the zero solution, and we look for an exponential growth of the perturbations. For a *generic* mode $\mathbf{k}$ the evolution equation of its perturbation δB is given by $\partial_\tau\delta B=\mu\,\delta B$, where $\mu=r-1-2\alpha^2$, and hence this mode becomes linearly unstable at $r=1+2\alpha^2$. However, if there exist two modes with wave vectors $\mathbf{k}_{\mathrm{I}}$ and $\mathbf{k}_{\mathrm{II}}$ satisfying the *phase-matching* (or resonance) condition

$$\mathbf{k}_{\mathrm{I}}+\mathbf{k}_{\mathrm{II}}=2\mathbf{k}_0, \tag{9}$$

the linearized equations for their perturbations $\delta B_{\mathrm{I}}, \delta B_{\mathrm{II}}$ are coupled, and are given by

$$\partial_\tau\delta B_{\mathrm{I}}=\mu\,\delta B_{\mathrm{I}}-\alpha^2\delta B_{\mathrm{II}}^{*}, \tag{10a}$$

$$\partial_\tau\delta B_{\mathrm{II}}=\mu\,\delta B_{\mathrm{II}}-\alpha^2\delta B_{\mathrm{I}}^{*}. \tag{10b}$$

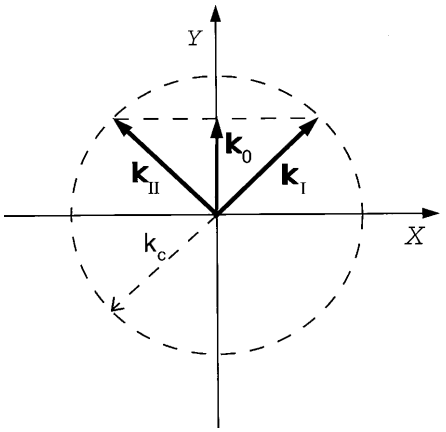

FIG. 1. The phase-matching condition (9).

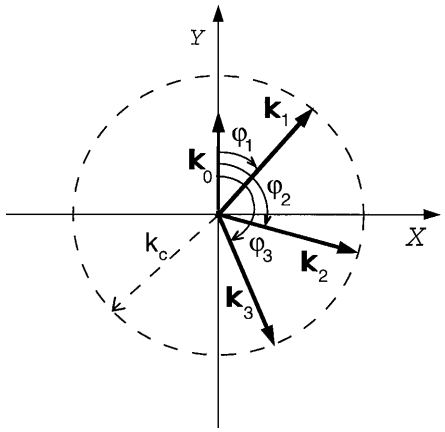

FIG. 2. The phase-matching conditions (11).

The eigenvalues associated with Eqs. (10) are $\lambda_{\pm}=\mu\pm\alpha^2$; hence these modes become linearly unstable at $r=1+\alpha^2$. The phase-matching condition (9), which is responsible for a threshold lowering for pattern formation, is shown in Fig. 1. It is clear that it can be satisfied only if $k_0<k_C$, and that if this is the case the wave vectors $\mathbf{k}_I$ and $\mathbf{k}_{II}$ are uniquely determined. In conclusion, the forced solution becomes linearly unstable at $r=1+\alpha^2$ if $k_0<k_C$, and at $r=1+2\alpha^2$ in the opposite case. These are the threshold values for the formation of patterns.

B. Stripe S_1 pattern ($N=1$)

For $r>1+2\alpha^2$ the amplitude equations (6) admit a family of solutions consisting of a single mode with wave vector, let us say, $\mathbf{k}_1$, having an arbitrary orientation and with amplitude $B_1=\sqrt{\mu}$, where $\mu=r-1-2\alpha^2$. If there exist wave vectors $\mathbf{k}_I$ and $\mathbf{k}_{II}$ satisfying the phase-matching condition (9), we require $\mathbf{k}_1\neq\mathbf{k}_I,\mathbf{k}_{II}$. In order to investigate the stability of this solution, we linearize Eqs. (9) around the steady-state solution $B_1=\sqrt{\mu}$, $B_2=B_3=\cdots=0$, and look for exponential growth of the perturbations. It turns out that perturbations associated with modes with a *generic* wave vector $\mathbf{k}$ are damped out, whereas two kinds of instabilities may arise for perturbations corresponding to wave vectors satisfying particular phase-matching conditions. The first source of instability is represented by the modes with wave vectors $\mathbf{k}_I$ and $\mathbf{k}_{II}$ satisfying the phase-matching condition (9), and it is easy to show that stability of the $\mathbf{S}_1$ solution against the growth of such modes requires $r>1+3\alpha^2$. The second source of instability, which is more restrictive, may arise for perturbations associated with the pair of wave vectors $\mathbf{k}_2$ and $\mathbf{k}_3$ satisfying one of the following *phase-matching* conditions:

$$\mathbf{k}_1+\mathbf{k}_2-\mathbf{k}_3=\mathbf{k}_0 \tag{11a}$$

or

$$\mathbf{k}_2+\mathbf{k}_3-\mathbf{k}_1=\mathbf{k}_0\,. \tag{11b}$$

In this case, assuming for instance that Eq. (11a) is satisfied, the linearized equations for the perturbations δB_2 and δB_3 read

$$\partial_\tau\delta B_2=-\mu\,\delta B_2-2\alpha\sqrt{\mu}\,\delta B_3\,, \tag{12a}$$

$$\partial_\tau\delta B_3=-\mu\,\delta B_3-2\alpha\sqrt{\mu}\,\delta B_2\,. \tag{12b}$$

The eigenvalues of the linearized Eqs. (12) are $\lambda_{\pm}=-\mu\pm2\alpha\sqrt{\mu}$; hence the stability of the $\mathbf{S}_1$ solution in this case requires $r>1+6\alpha^2$. As the phase-matching conditions (11) play an important role in destabilizing the $\mathbf{S}_1$ patterns, it is of interest to study under which conditions they can be satisfied. The phase matching conditions (11) are sketched in Fig. 2; with the notations shown in the figure, it is straightforward to show that the wave vectors $\mathbf{k}_2$ and $\mathbf{k}_3$ satisfying Eq. (11a) are determined by the angles φ_2 and φ_3 given by

$$\varphi_{2,3}=\arctan\left[\frac{\gamma-\cos\varphi_1}{\sin\varphi_1}\right]\pm\arcsin\left[\frac{1+\gamma^2-2\gamma\,\cos\varphi_1}{4}\right]^{1/2}, \tag{13}$$

where φ_1 is the angle between the wave vectors $\mathbf{k}_1$ and $\mathbf{k}_0$, and $\gamma=k_0/k_C$. For the phase-matching condition (11b), Eq. (13) is still valid provided that the substitution $\varphi_1\to\varphi_1+\pi$ is made. In order that at least one of the two phase-matching conditions (11) be satisfied for *any* value of the angle φ_1, the condition $k_0<\sqrt{3}k_C$ must be fulfilled. When $k_0>3k_C$ the phase-matching conditions may never be satisfied, whereas for $\sqrt{3}k_C<k_0<3k_C$ one of the two phase-matching conditions (11) may be satisfied for the $\mathbf{S}_1$ solutions, whose wave vectors $\mathbf{k}_1$ fall inside the cone shown in Fig. 3. As shown in Fig. 4, the transverse intensity profile for the $\mathbf{S}_1$ pattern corresponds to stripes whose orientation and spatial period depend upon the angle φ_1 between the wave vectors $\mathbf{k}_1$ and $\mathbf{k}_0$. In conclusion, we can say that a family of $\mathbf{S}_1$ patterns exists for $r>1+2\alpha^2$, and their stability is governed by the following rules: (1) when $k_0<\sqrt{3}k_C$ all the $\mathbf{S}_1$ patterns are stable for $r>1+6\alpha^2$, and unstable otherwise; (2) when $\sqrt{3}k_C<k_0<3k_C$, stability of the $\mathbf{S}_1$ patterns whose wave vectors fall inside the cone shown in Fig. 3 is ruled as in (1), the other patterns being always stable; and (3) when $k_0>3k_C$ the $\mathbf{S}_1$ patterns are always stable in their domain of existence.

C. Stripe S_2 patterns ($N=2$)

The amplitude equations (6) have a family of solutions corresponding to the excitation of two tilted waves with wave vectors $\mathbf{k}_1$ and $\mathbf{k}_2$. However, as in the laser case with-

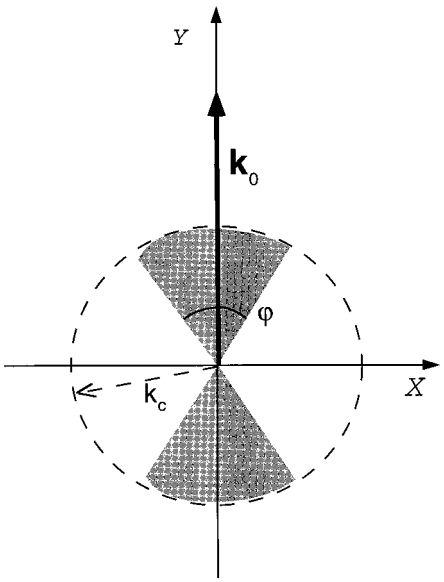

FIG. 3. The phase-matching conditions (11) in the case $\sqrt{3}k_0 < k_C < 3k_0$ may be satisfied only for the wave vectors $\mathbf{k}_1$ which fall inside the shaded cone oriented along $\mathbf{k}_0$, with aperture angle $\varphi = \arccos((\gamma^2-3)/2\gamma)$.

out injected signal [7], it turns out that such solutions are unstable for a *generic* pair of wave vectors. When the signal is injected into the cavity, stable two-wave solutions may nevertheless occur when the phase-matching condition (9) is satisfied. In this case the amplitude equations for the modes with wave vectors $\mathbf{k}_{\mathrm{I}}$ and $\mathbf{k}_{\mathrm{II}}$ are given by

$$\partial_\tau B_{\mathrm{I}} = \mu B_{\mathrm{I}} - (|B_{\mathrm{I}}|^2 + 2|B_{\mathrm{II}}|^2)B_{\mathrm{I}} - \alpha^2 B_{\mathrm{II}}^*, \qquad (14a)$$

$$\partial_\tau B_{\mathrm{II}} = \mu B_{\mathrm{II}} - (|B_{\mathrm{II}}|^2 + 2|B_{\mathrm{I}}|^2)B_{\mathrm{II}} - \alpha^2 B_{\mathrm{I}}^*, \qquad (14b)$$

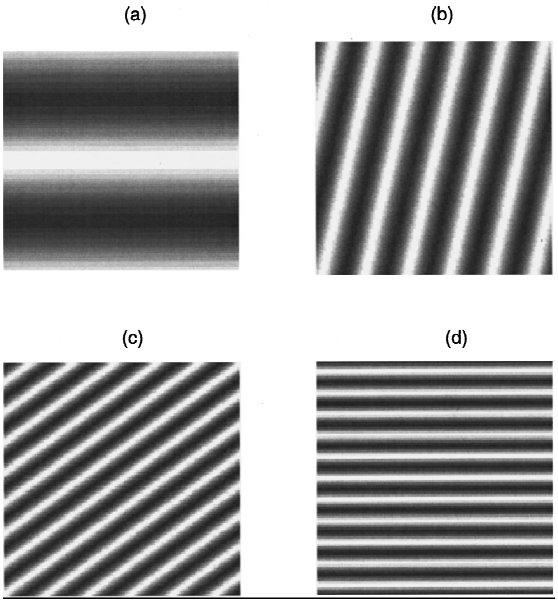

FIG. 4. Snapshots of stable $\mathbf{S}_1$ stripe patterns corresponding to four different values of the angle φ_1: (a) $\varphi_1 = 0$, (b) $\varphi_1 = \pi/3$, (c) $\varphi_1 = 2\pi/3$, and (d) $\varphi_1 = \pi$. The values of the other parameters are $k_C = 1$, $k_0 = 0.7$, $\alpha = 1$, and $r = 13$. Here and in the following figures the wave vector $\mathbf{k_0}$ is oriented along the vertical direction.

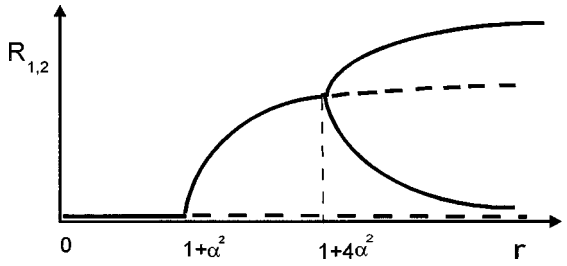

FIG. 5. Bifurcation diagram for the $\mathbf{S_2}$ patterns. The symmetric solution ($R_1 = R_2$) is stable for $1+\alpha^2 < r < 1+4\alpha^2$, whereas the asymmetric solution ($R_1 \neq R_2$) is stable for $r > 1+4\alpha^2$. The solid (dashed) lines correspond to stable (unstable) solutions.

where the last terms on the right-hand side in Eqs. (14) arise in consequence of the phase-matching condition (9). In order to investigate the bifurcation properties of these equations, let us introduce the polar decomposition $B_{\mathrm{I}} = R_1 \exp(i\phi_1)$, $B_{\mathrm{II}} = R_2 \exp(i\phi_2)$ and the phase variable $\phi = \phi_1 + \phi_2$, so that Eqs. (14) become

$$\partial_\tau R_1 = \mu R_1 - (R_1^2 + 2R_2^2)R_1 - \alpha^2 R_2 \cos\phi, \qquad (15a)$$

$$\partial_\tau R_2 = \mu R_2 - (R_2^2 + 2R_1^2)R_2 - \alpha^2 R_1 \cos\phi, \qquad (15b)$$

$$\partial_\tau \phi = \alpha^2 \left(\frac{R_1^2 + R_2^2}{R_1 R_2} \right) \sin\phi. \qquad (15c)$$

From Eq. (15c) it follows that, apart from the trivial zero solution (corresponding to the forced-mode state previously investigated), the steady-state solutions are phase locked and correspond to $\sin\phi = 0$, i.e., to $\phi = \pi$ or to $\phi = 0$. The latter solution is, however, always unstable to phase fluctuations, and therefore here we will consider only the case $\phi = \pi$. The equations for the real amplitudes [Eqs. (15a) and (15b)] then have two kinds of solutions: the symmetric solution $\mathbf{S}_{2S}$, corresponding to

$$R_1 = R_2 = \left(\frac{\mu + \alpha^2}{3} \right)^{1/2}, \qquad (16)$$

and the asymmetric solution $\mathbf{S}_{2A}$, given by

$$R_{1,2} = \left(\frac{\mu \pm \sqrt{\mu^2 - 4\alpha^4}}{2} \right)^{1/2}. \qquad (17)$$

The symmetric solution (16) exists for $r > 1+\alpha^2$ whereas the asymmetric solution (17) exists for $r > 1+4\alpha^2$. Straightforward linearization of the dynamical equations (15a) and (15b) around these steady-state solutions indicates that the symmetric solution is stable for $r < 1+4\alpha^2$. At $r = 1+4\alpha^2$ a bifurcation takes place, resulting in the stability of the asymmetric solution. The bifurcation diagram for the two-wave equations (14) is shown in Fig. 5. These stability criteria consider only the nonlinear interaction between the modes $\mathbf{k}_{\mathrm{I}}$ and $\mathbf{k}_{\mathrm{II}}$; however, it may be shown that they are still valid when considering the linear stability problem within the full amplitude equations (6) [33]. In particular, it turns out that the $\mathbf{S}_2$ patterns are always stable with respect to external perturbations for which the phase-matching condition (11) (with $\mathbf{k}_1 = \mathbf{k}_{\mathrm{I}}, \mathbf{k}_{\mathrm{II}}$) is valid. The $\mathbf{S}_2$ patterns corresponding to

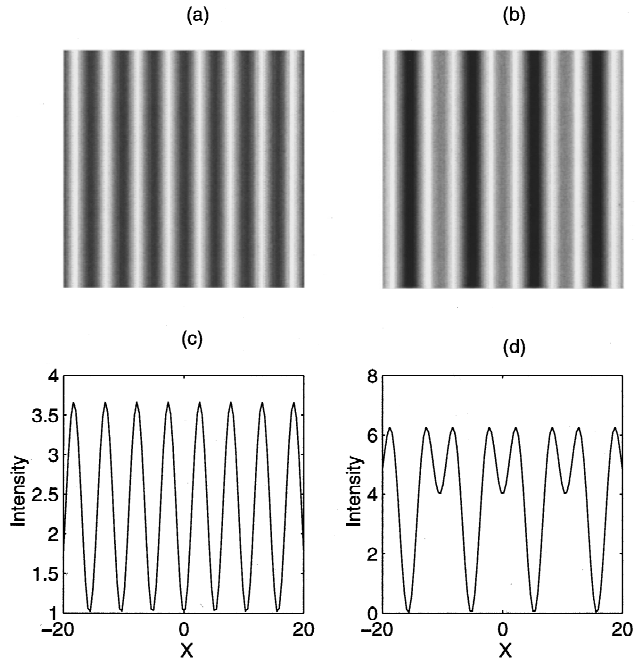

FIG. 6. Snapshots [(a) and (b)] and corresponding intensity profiles [(c) and (d)] of the $\mathbf{S}_2$ stripe patterns. (a) and (c) correspond to the symmetric solution ($r=4$), whereas (b) and (d) correspond to the asymmetric solution ($r=6$). The values of the other parameters are $k_C=1$, $k_0=0.8$, and $\alpha=1$.

the two-wave solutions (16) and (17) are shown in Fig. 6. The $\mathbf{S}_{2S}$ solution corresponds to stripes parallel to the wave vector $\mathbf{k}_0$ with a single spatial periodicity, whereas the $\mathbf{S}_{2A}$ solution gives rise to stripes parallel to $\mathbf{k}_0$ but with a double spatial periodicity (see Fig. 6). It is remarkable the fact that, although the final intensity pattern arises from the interference of three different traveling waves [with wave vectors $\mathbf{k}_0$, $\mathbf{k}_{\mathrm{I}}$, and $\mathbf{k}_{\mathrm{II}}$; see Eq. (8)], it corresponds to stripes. This feature is a consequence of the phase-matching condition (9), which physically is imposed by the conservation of the photon momentum in the nonlinear interaction process of the three waves. Although the resonance condition (9) among the wave vectors of the different TW's is fundamental in determining the final pattern as in other optical systems (such as in the multiconical emission [20,25]), it is interesting to observe that in our case there is only partial phase locking among these modes. In fact, in the stable steady-state pattern what is fixed is only the sum $\phi_1+\phi_2$ of the phases of modes $\mathbf{k}_{\mathrm{I}}$ and $\mathbf{k}_{\mathrm{II}}$ (with respect to the reference phase of $\mathbf{k}_0$ which was assumed to be zero), leaving undetermined either ϕ_1 or ϕ_2. In conclusion, the $\mathbf{S}_2$ patterns exist when $k_0<k_C$, and their existence and stability domains are summarized in the bifurcation diagram shown in Fig. 5.

D. Undulating hexagons ($N=3$)

The amplitude equations (6) admit of a family of solutions corresponding to the excitation of three tilted waves. In general, it turns out that a steady-state solution of the amplitude equations (6) involving three modes $\mathbf{k}_1$, $\mathbf{k}_2$, and $\mathbf{k}_3$ is unstable unless the phase-matching condition (11a) [or (11b)] for these modes is satisfied. In this case, assuming for instance that the phase-matching condition (11a) is satisfied, the amplitude equations for the three modes read explicitly as [34]

$$\partial_\tau B_1=\mu B_1-(|B_1|^2+2|B_2|^2+2|B_3|^2)B_1-2\alpha B_3B_2^*, \tag{18a}$$

$$\partial_\tau B_2=\mu B_2-(|B_2|^2+2|B_1|^2+2|B_3|^2)B_2-2\alpha B_3B_1^*, \tag{18b}$$

$$\partial_\tau B_3=\mu B_3-(|B_3|^2+2|B_1|^2+2|B_2|^2)B_3-2\alpha B_1B_2. \tag{18c}$$

These equations have a canonical form as they typically describe the roll-hexagon competition in systems with a second-order nonlinearity [15,35]. In particular, they have also become quite standard in the optical context to describe roll-hexagon transition in passive Kerr-like systems [2–4]. Note, however, that in the present context they govern the dynamics of three single TW's on the critical circle, and not of six TW's as in previous models [2–4]. Nevertheless, as the bifurcation properties of these equations are well known, here we will report only the result of the analysis. Introducing the polar decomposition $B_l=R_l\exp(i\phi_l)$ ($l=1$, 2, and 3) and the phase variable $\phi=\phi_1+\phi_2-\phi_3$, it turns out that, within the dynamical model expressed by Eqs. (18), the phase-locked solution with $\phi=\pi$ is the only stable solution with respect to phase fluctuations; the steady-state amplitudes for the three waves is then composed by two branches, given by

$$R_1=R_2=R_3\equiv R=\frac{\alpha\pm\sqrt{\alpha^2+5\mu}}{5}. \tag{19}$$

The lower branch [corresponding to the lower sign in Eq. (19)] is always unstable in its domain of existence, whereas it turns out that the upper branch is stable for $-\alpha^2/5<\mu<16\alpha^2$ [35]. The typical patterns arising from the interference of these three waves with the forced mode are shown in Fig. 7 for a few values of the angle φ_1, which is the free family parameter. As it can be seen, these patterns correspond to lattices of hexagons in the ''inverted'' configuration analogous to those found in optical bistability [17]. However, in our case these hexagons are distorted, and we will call them undulating hexagons. As previously observed for the $\mathbf{S}_2$ patterns, the hexagonal nature of the patterns is closely related to the phase matching condition (11), and the final tiling requires only partial locking of phases of the modes. The distorted shape of the hexagons, instead, is a consequence of the fact that they arise as a superposition of *traveling waves* whose orientation in space is governed by Eqs. (11), and not of *rolls* as in the optical bistability. As a final remark, it should be noted that a global stability analysis of the hexagonal patterns must be done within the full amplitude equations (6) as other modes not considered in Eqs. (18) may become unstable [33]. A linear stability analysis of the hexagonal patterns with respect to external perturbations shows that a source of instability may arise when considering perturbations for the modes $\mathbf{k}_{\mathrm{I}}$ and $\mathbf{k}_{\mathrm{II}}$ satisfying the phase-matching condition (9). In this case the linearized equations which describe the evolution of the perturbations read

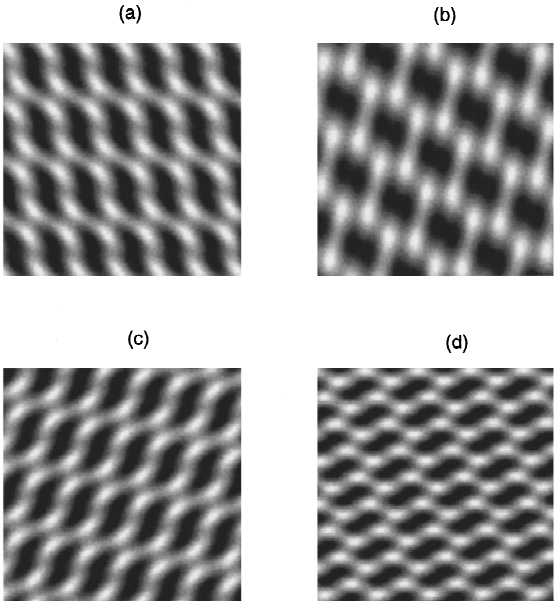

FIG. 7. Snapshots of stable undulating hexagons for four values of the angle φ_1: (a) $\varphi_1=0$, (b) $\varphi_1=\pi/3$, (c) $\varphi_1=2\pi/3$, and (d) $\varphi_1=\pi$. The values of the other parameters are $k_C=1$, $k_0=0.4$, $\alpha=1$, and $r=3.1$.

$$\partial_\tau \delta B_{\mathrm{I}} = (\mu - 6R^2)\,\delta B_{\mathrm{I}} - \alpha^2\,\delta B_{\mathrm{II}}^*\,, \tag{20a}$$

$$\partial_\tau \delta B_{\mathrm{II}} = (\mu - 6R^2)\,\delta B_{\mathrm{II}} - \alpha^2\,\delta B_{\mathrm{I}}^*\,. \tag{20b}$$

The eigenvalues of Eqs. (20) are $\lambda_\pm = \mu - 6R^2 \pm \alpha^2$. Stability of the hexagonal lattice against the growth of the $\mathbf{S}_2$ modes requires therefore $\mu - 6R^2 + \alpha^2 < 0$ which, using Eq. (19), reads explicitly as $r > 1 + 2.0294\ldots\alpha^2$.

In conclusion, hexagonal patterns exist when $k_0 < 3k_C$ and they are stable for $1 + 2.0294\ldots\alpha^2 < r < 1 + 18\alpha^2$ if $k_0 < k_C$, and for $1 + 9\alpha^2/5 < r < 1 + 18\alpha^2$ otherwise. The stability properties of the patterns at different tilting angles of the injected signal are summarized in Table I and Fig. 8.

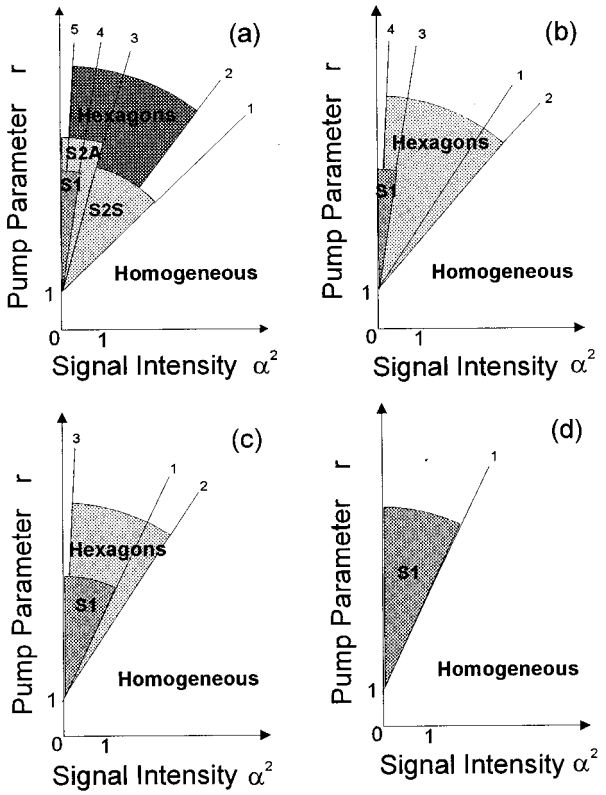

FIG. 8. Stability domains of the different patterns in the (α^2, r) plane for (a) $0 < k_0 < k_C$, (b) $k_C < k_0 < \sqrt{3}k_C$, (c) $\sqrt{3}k_C < k_0 < 3k_C$, and (d) $k_0 > 3k_C$. The forced (homogeneous) mode is stable below line 1, whereas the other patterns are linearly stable in infinitely extended cones whose vertex is (0,1). These cones are delimited on the left and on the right sides by the lines 1,2,3, . . . for the different patterns, as ruled in Table I. Overlapping regions of the cones indicate multistability.

IV. PATTERN SELECTION AND CONTROL

The various transverse patterns studied in Sec. III may appear in the laser emission when the control parameters are varied. Typically in our physical system there are three control parameters that one can vary: the pumping parameter r; the normalized amplitude of the injected signal, α; and the tilting angle of the injected signal with respect to the cavity axis, i.e., k_0. As a general rule, from Table I and Fig. 8 it turns out that at high values of the pump parameter only *one tilted wave* is excited independently of the tilting angle of the

TABLE I. Summary of the stability domains of the various patterns for different values of the transverse wave vector k_0 of the injected signal. The control parameter $\alpha \equiv B_0$, given by Eq. (7), is proportional to the amplitude of the injected signal.

	$0<k_0<k_C$	$k_C<k_0<\sqrt{3}k_C$	$\sqrt{3}k_C<k_0<3k_C$	$k_0>3k_C$
Forced mode ($N=0$)	$r<1+\alpha^2$	$r<1+2\alpha^2$	$r<1+2\alpha^2$	$r<1+2\alpha^2$
S_1 patterns ($N=1$)	$r>1+6\alpha^2$	$r>1+6\alpha^2$	$r>1+6\alpha^2$ or $r>1+2\alpha^2$	$r>1+2\alpha^2$
S_{2S} patterns ($N=2$)	$1+\alpha^2<r<1+4\alpha^2$			
S_{2A} patterns ($N=2$)	$r>1+4\alpha^2$			
Hexagonal patterns ($N=3$)	$1+2.0294\cdots\alpha^2<r<1+18\alpha^2$	$1+9\alpha^2/5<r<1+18\alpha^2$	$1+9\alpha^2/5<r<1+18\alpha^2$	

injected field, and the laser output intensity tends to be uniform in space. We therefore recover a characteristic property of the laser emission without injected signal. Conversely, at high values of the injected signal the laser emission always occurs in the forced mode, and all the tilted waves are suppressed as the gain saturation introduced by the forced mode does not allow these modes to reach threshold for oscillation. For intermediate values of the control parameters the laser emission occurs in more complicated patterns, and a sequence of bifurcations connecting the two limiting situations takes place. Here we will consider a fixed amplitude of the injected signal, and will study the bifurcation scenario which appears when the pump parameter is varied at different tilting angles of the injected signal. A similar analysis could, however, be done by considering a fixed value of the pump parameter, and assuming that the amplitude of the injected signal is a bifurcation parameter. According to the analysis developed in Sec. III, four cases have to be distinguished.

A. Case I: $k_0 < k_C$

The laser emits in the forced (homogeneous) mode for $r < 1+\alpha^2$, and the threshold for pattern formation is reached at $r=1+\alpha^2$, where the symmetric stripe pattern $\mathbf{S}_{2S}$ bifurcates supercritically from the homogeneous mode. At $r=1+4\alpha^2$ a second bifurcation takes place with the appearance of the double-period stripe pattern $\mathbf{S}_{2A}$, which remains stable at higher values of the pump parameter (see Fig. 5). $\mathbf{S}_1$ stripe patterns and hexagons may also be observed for $k_0 < k_C$, their domains of stability being $r > 1+6\alpha^2$ for stripes and $1+2.0294\ldots\alpha^2 < r < 1+18\alpha^2$ for hexagons, respectively. Therefore bistability and even tristability of patterns may exists in this case in some ranges of the pumping parameter [see Fig. 8(a)]. It should be noted that, at high values of the pump parameter, the two stable states $\mathbf{S}_{2A}$ and $\mathbf{S}_1$ correspond both to the excitation of *one* tilted wave, and the transverse output intensity tends to be uniform in space.

B. Case II: $k_C < k_0 < \sqrt{3} k_C$

In this case the stable laser oscillation is in the forced state for $r < 1+2\alpha^2$, and, at $r=1+2\alpha^2$, a subcritical bifurcation leading to the emergence of hexagonal patterns takes place. The hexagonal lattice looses its stability at $r=1+18\alpha^2$, where a second bifurcation and a transition to $\mathbf{S}_1$ stripe patterns appear. Bistability between the homogeneous mode and the hexagonal lattice, and between the hexagonal lattice and the $\mathbf{S}_1$ patterns, exist for $1+9\alpha^2/5 < r < 1+2\alpha^2$ and $1+6\alpha^2 < r < 1+18\alpha^2$, respectively.

C. Case III: $k_0 > 3k_C$

As in case II, the laser emission occurs on the forced mode for $r < 1+2\alpha^2$. At $r=1+2\alpha^2$ a supercritical bifurcation leading to the emergence of a stripe pattern $\mathbf{S}_1$ occurs, which remains stable at higher values of the pump parameter. This bifurcation scenario is analogous to that of a laser with a detuned injected signal studied in Ref. [31].

D. Case IV: $\sqrt{3} k_C < k_0 < 3k_C$

In this case either one of the two bifurcation scenarios discussed in cases II or III may occur, and which one will occur depends upon the tilted wave mode selected by the noise at the bifurcation point. In particular, any tilted wave whose wave vector falls inside the cone shown in Fig. 3 will give the bifurcation scenario described in case II.

V. CONCLUSION AND DISCUSSION

In this paper we have investigated theoretically the emergence of transverse patterns in a large-aspect-ratio, single-longitudinal-mode laser in the positive detuning case under the action of a weak, plane-wave-injected signal tilted with respect to the axis of the laser cavity. As the longitudinal cavity frequency is smaller than the atomic transition frequency, the laser emission spontaneously occurs off-axis. The continuum of bifurcating modes are tilted waves whose frequency exactly coincides with the atomic transition frequency and whose transverse wave vectors are fixed (in modulus) by the detuning parameter [7]. In the absence of the injected signal, it is known that the laser dynamics typically selects one tilted wave, which is able to suppress all others [7]. As shown in Ref. [31], this scenario is, in general, maintained even when a signal field is injected into the laser cavity, with the only difference that the selected tilted wave is superimposed to the forced mode of the laser equations. In this paper we have shown that, when the frequency of the injected signal is exactly tuned to the atomic transition frequency, new resonances appear in the amplitude equations, which drastically change the pattern forming properties of the free-running laser. This leads to the formation of new stable patterns. In particular, it has been shown that stable patterns arising from the superposition of the forced mode with one, two, or three tilted waves may occur, and that these patterns may be conveniently selected by varying the pumping parameter and the angle of the injected signal from the cavity axis. Even close to threshold, where the amplitude equations may correctly describe the laser dynamics, it has been shown that a rich sequence of bifurcations takes place connecting the two limiting dynamical regimes corresponding to the free-running laser and to stable oscillation on the forced mode. Similar patterns and bifurcations appear in the study of passive optical systems, such as Kerr-like media with two-dimensional feedback [3], multiconical emission [23–26], and thin two-level media with delayed feedback [28], which we discussed in Sec. I. In particular, the occurrence of resonance conditions [like those expressed by Eqs. (9) and (11)] among different critical modes are common in the study of quasipatterns [19] and of multiconical emission [23,25,26]. Our analysis hence extends to an active optical system some pattern features which were considered to be peculiar to passive systems. Nevertheless, in our context there are some distinctive and new aspects that should be pointed out. As discussed in Sec. I, the elementary patterns are different in active and passive systems: traveling waves in the first class of systems, standing waves (rolls) in the second one [16]. This fact has important consequences on pattern formation in the two types of systems, which become evident in the analysis of the far-field patterns. To better understand this point, let us observe, for example, that undulating hexagonal patterns like those shown in Fig. 7 are very similar to other hexagonal patterns observed in passive systems (see, for instance, Fig. 5 of Ref. [28]). Although they

arise in both cases in consequence of resonance conditions [a four-wave interaction ruled by Eqs. (11) in our system, a triadic Turing-Hopf interaction in the model of Ref. [28]], the far-field patterns are different in the two cases. In the model of Ref. [28] the far-field pattern is composed of six spots with the symmetry $\mathbf{k}\rightarrow-\mathbf{k}$, which is imposed by the conservation of the transverse photon momentum in the elementary process of pattern formation; conversely, this symmetry is broken in the laser case, where the far-field pattern is composed only of four spots (see Fig. 2). Furthermore, as discussed in Sec. III, phase locking among the excited TW's is only partial in our model, whereas it seems to be fundamental in other passive systems [26]. Another interesting and distinctive feature is the bifurcation between $\mathbf{S}_{2S}$ and $\mathbf{S}_{2A}$ patterns studied in Sec. III, where TW's with different intensities may be excited. This bifurcation is analogous to that studied in hydrodynamics in oscillatory convection [36], and corresponds, using hydrodynamic terminology, to a transition from standing to mixed traveling waves [36,37].

A singular configuration, which has not been studied here, is that of normal incidence of the injected signal. In this geometry the rotational symmetry of the laser equations in the transverse plane is restored, and this introduces in the amplitude equations special resonances that are absent in the tilted case. In particular, the effect of these resonances is to prevent the existence of solutions for the amplitude equations (6) composed of an odd number of traveling waves on the critical circle as two opposite traveling waves are always linearly coupled. Nevertheless, these coupled TW's may have different amplitudes. Another point that has to be discussed for its relevance from an experimental viewpoint is how the pattern formation rules here investigated change when the injected signal is detuned from the atomic transition frequency by an amount, let us say ϑ. It is clear that if ϑ is of order $O(1)$, the resonant terms in the amplitude equations responsible for the emergence of the new patterns disappear and the scenario described in Ref. [31] is recovered. On the contrary, when ϑ is small, i.e., for a slight detuning, the problem is nontrivial, and inclusion of finite bandwidth effects in the perturbation analysis developed in Sec. II becomes of fundamental importance. When including in the amplitude equations finite bandwidth effects, an annulus of modes of width of $O(\varepsilon)$ around $k_C=\sqrt{\Omega/a}$ in the $\mathbf{k}$ space enter into the dynamical equations [7], where the smallness parameter ε defines the order of magnitude of the forced mode in the cavity (see Sec. II). As a result of the dispersion relation for the traveling waves, the frequency of these modes covers an interval around the atomic transition frequency whose width is of $O(\varepsilon)$ [7]. Hence if ϑ is of the same order as ε, resonances in the amplitude equations may still occur and the pattern formation properties here investigated should be still valid. A detailed analysis of the detuned case, including the derivation of order parameter equations, will be given in a separate work [37].

[1] See, for instance, *Nonlinear Optical Structures, Patterns, Chaos*, edited by L. A. Lugiato, special issue of Chaos Solitons Fractals **4** (1994).

[2] W. J. Firth, J. Mod. Opt. **37**, 151 (1990); G. D'Alessandro and J. W. Firth, Phys. Rev. Lett. **66**, 2597 (1991).

[3] R. MacDonald and H. J. Eichler, Opt. Commun. **89**, 289 (1992); E. Pampaloni, S. Residóri, and F. T. Arecchi, Europhys. Lett. **24**, 647 (1993); G. Grynberg, A. Maitre, and A. Petrossian, Phys. Rev. Lett. **72**, 2379 (1994); G. D'Alessandro, E. Pampaloni, P.-L. Ramazza, S. Residori, and F. T. Arecchi, Phys. Rev. A **52**, 4176 (1995).

[4] W. J. Firth, A. J. Scroggie, G. S. McDonald, and L. A. Lugiato, Phys. Rev. A **46**, R3609 (1992); M. Tlidi, M. Georgiou, and P. Mandel, Phys. Rev. A **48**, 4605 (1993).

[5] D. Leduc, M. Le Berre, E. Ressayre, and A. Tallet, Phys. Rev. A **53**, 1072 (1996).

[6] F. Prati, M. Brambilla, and L. A. Lugiato, Riv. Nuovo Cimento **17**, 1 (1994).

[7] P. K. Jakobsen, J. V. Moloney, A. C. Newell, and R. Indik, Phys. Rev. A **45**, 8129 (1992); P. K. Jakobsen, J. Lega, Q. Feng, M. Staley, J. V. Moloney, and A. C. Newell, *ibid.* **49**, 4189 (1994); J. Lega, P. K. Jakobsen, J. V. Moloney, and A. C. Newell, *ibid.* **49**, 4201 (1994).

[8] J. Lega, J. V. Moloney, and A. C. Newell, Physica D **83**, 478 (1995).

[9] Q. Feng, J. V. Moloney, and A. C. Newell, Phys. Rev. A **50**, R3601 (1994); K. Staliunas and C. O. Weiss, Physica D **81**, 79 (1995).

[10] K. Staliunas, M. F. H. Tarroja, G. Slekys, C. O. Weiss, and L. Dambly, Phys. Rev. A **51**, 4140 (1995).

[11] F. T. Arecchi, S. Boccaletti, P. L. Ramazza, and S. Residori, Phys. Rev. Lett. **70**, 2277 (1993).

[12] G.-L. Oppo, M. Brambilla, and L. A. Lugiato, Phys. Rev. A **49**, 2028 (1994).

[13] S. Longhi, Phys. Rev. A **53**, 4488 (1996); J. Mod. Opt. **43**, 1569 (1996).

[14] G. J. deValcarcel, K. Staliunas, E. Roldan, and V. J. Sanchez-Morcillo, Phys. Rev. A **54**, 1609 (1996).

[15] M. C. Cross and P. C. Hohenberg, Rev. Mod. Phys. **65**, 851 (1993).

[16] J. B. Geddes, J. Lega, J. V. Moloney, R. A. Indik, E. M. Wright, and W. J. Firth, Chaos Solitons Fractals **4**, 1261 (1994).

[17] W. J. Firth and A. J. Scroggie, Europhys. Lett. **26**, 521 (1994).

[18] M. Tlidi, R. Lefever, and P. Mandel, Quantum Semiclassic. Opt. **8**, 931 (1996).

[19] H. W. Muller, Phys. Rev. E **49**, 1273 (1994).

[20] B. Christiansen, P. Alstrom, and M. T. Levinsen, Phys. Rev. Lett. **68**, 2157 (1992); W. S. Edwards and S. Fauve, Phys. Rev. E **47**, R788 (1993).

[21] D. Lima, A. De Wit, G. Dewel, and P. Borckmans, Phys. Rev. E **53**, R1305 (1996).

[22] E. Pampaloni, P.-L. Ramazza, S. Residori, and F. T. Arecchi, Phys. Rev. Lett. **74**, 258 (1995).

[23] E. V. Degtiarev and M. A. Vorontsov, J. Mod. Opt. **43**, 93 (1996); M. A. Vorontsov and A. Y. Karpov, J. Opt. Soc. Am. B **14**, 34 (1997).

[24] A. A. Afanas'ev and B. A. Samson, Phys. Rev. A **53**, 591 (1996).

[25] M. Le Berre, D. Leduc, E. Ressayre, and A. Tallet, Phys. Rev. A **54**, 3428 (1996).
[26] E. Pampaloni, S. Residori, S. Soria, and F. T. Arecchi, Phys. Rev. Lett. **78**, 1042 (1997).
[27] S. Residori, P. L. Ramazza, E. Pampaloni, S. Boccaletti, and F. T. Arecchi, Phys. Rev. Lett. **76**, 1063 (1996).
[28] Y. A. Logvin, B. A. Samson, A. A. Afanas'ev, A. M. Samson, and N. A. Loiko, Phys. Rev. E **54**, R4548 (1996).
[29] See, for instance, the special feature on instabilities in active optical media, J. Opt. Soc. Am. B **2**, 5 (1985).
[30] Paul Mandel, M. Georgiou, and T. Erneux, Phys. Rev. A **47**, 4277 (1993).
[31] M. Georgiou and Paul Mandel, Chaos Solitons Fractals **4**, 1657 (1994).
[32] In the singular limit $k_0=k_C$ the right scaling for the pump parameter and for the injected signal is $r=1+\varepsilon^2$, $E=O(\varepsilon^3)$; see also Ref. [20]. In this case the effect of the injected signal is merely to force the laser emission in the tilted wave mode corresponding to the injected signal.
[33] The linear stability analysis of a pattern has to be done, in general, by considering both perturbations of modes belonging to the pattern (*internal perturbations*) and perturbations of modes which do not belong to the pattern (*external perturbations*). The stability analysis with respect to external perturbations governs the competition among patterns belonging to different families. See B. A. Malomed, A. A. Nepomnyashchii, and M. I. Tribelskii, Zh. Eksp. Teor. Fiz. **96**, 684 (1989) [Sov. Phys. JETP **69**, 388 (1989)].
[34] If $k_0<k_C$ we require $\mathbf{k}_l\neq K_{I,II}$ for $l=1$, 2, and 3.
[35] S. Ciliberto, P. Coullet, J. Lega, E. Pampaloni, and C. Perez-Garcia, Phys. Rev. Lett. **65**, 2370 (1990).
[36] H. Riecke, J. D. Crawford, and E. Knobloch, Phys. Rev. Lett. **61**, 1942 (1988).
[37] S. Longhi, Phys. Rev. A (to be published).